1

Novel Actuation Methods for High Force Haptics

Stephen P. Buerger and Neville Hogan
Massachusetts Institute of Technology
United States of America

1. Introduction

Most haptic devices are intended primarily, if not exclusively, to exchange information with a human operator, and often replace or augment traditional computer displays with backdrivable, force-producing tactile interfaces. This includes popular commercial devices such as the PHANTOM (Massie & Salisbury, 1994) that are typically limited to at most several Newtons of endpoint force capacity, just enough to display simple virtual environments to the operator. Less conventional wearable haptic devices operate differently, but similarly have a low force capacity sufficient only to convey information (e.g. see devices described in (Biggs & Srinivasan, 2002)). By contrast, a class of applications that we refer to as *high force haptics* requires devices that exchange significant forces (and sometimes power) with an operator, often up to and exceeding the force to move limbs or even large fractions of body weight. While achieving high forces, these devices must also present low mechanical endpoint impedance to the operator (i.e. be backdrivable or feel "gentle") in order to avoid injury and, frequently, to exchange information with the operator by representing virtual environments. We propose the following working definition:

> *High force haptic device:* A mechanical device for physical interaction with humans in one or more degrees of freedom that can actively produce controlled force and motion comparable to the capability of the limbs it interacts with and can be back-driven over the same motion range by forces much less than the capacity of the same limbs.

This definition is not intended to be rigid or comprehensive but to provide a framework to elucidate the challenges of developing devices with high force capacity and low mechanical endpoint impedance capable of rendering virtual environments. "Force" and "motion" are considered here to be generalized quantities that include force and position as well as their derivatives or integrals, which are often important. For instance, velocity is important to accommodate typical limb motion, and the rate of change of force is important to display impact-like experiences. This applies to controlled outputs from the devices as well as to backdriving. "Comparable to" means exceeding X% of (force and motion capabilities of relevant limbs), where X is as close to 100 as practical—often tens to hundreds of Newtons or more. "Much less than" means less than Y%, where $Y << X$; in fact the ratio X/Y is a key measure of high force haptic performance, and maximizing this ratio is the central challenge.

The application of robots to provide sensory-motor physiotherapy is a flagship application of high force haptics, and provides an instructive example of the engineering challenges unique to this emerging area. The ultimate goal is to promote, enhance and accelerate recovery after any injury that affects motor behavior. Common examples include stroke (cerebral vascular accident) (Volpe et al., 2009) and cerebral palsy (Krebs et al., 2009). Scientific and clinical evidence has shown that movement of the affected limbs is a key element of the recovery process. The compromised ability to move that immediately follows injury such as stroke may lead to permanent motor disability if left unaddressed, even though the peripheral neural, muscular and skeletal system is intact, a phenomenon that has been termed "learned non-use" (Taub and Uswatte, 2006; Wolf et al., 2006). In the case of cerebral palsy, unaddressed motor deficits also interfere with a child's development, leading to severe, permanent motor disability. In contrast, studies (Nudo, 2007) have shown that activity-dependent neural plasticity can offset these degenerative trends and, in some cases, even reverse them.

The process of recovery resembles motor learning (Hogan et al., 2006) though there are notable differences, such as abnormal muscle tone or spasticity, that do not occur in motor learning. Providing a high "dosage" or "intensity" of movement experience (many repetitions) is one of the ways robotic tools may augment conventional physiotherapy. However, repetition alone is not enough: voluntary participation is essential (Volpe et al., 2004). To ensure voluntary participation, the machine must assist only as needed. Even more important, the machine must not suppress any productive movements a patient can make. It must "get out of the way" of appropriate movements while gently resisting inappropriate movements; *guidance* is more important than *assistance* (Krebs et al., 2003). The requirement to provide permissive guidance—encouraging "good" movements while discouraging "bad" movements—is perhaps the most important distinction between therapeutic robotics and assistive technologies such as amputation prostheses, powered orthoses, etc. The latter compensate for a motor deficit; the former attempt to ameliorate it.

This may account for the contrasting results to date with upper-extremity and lower-extremity robotic therapy. Robotic treatment of upper-extremity stroke-related motor disorders has consistently succeeded, typically providing more than twice the benefit of conventional therapy alone (Kwakkel et al., 2007; Prange et al., 2006). It has even proven beneficial for stroke survivors in the "chronic phase", many years after injury, when all recovery had apparently ceased. In contrast, clinical studies to date have shown that robotic treatment of lower-extremity motor disorders is about half as effective as conventional approaches (Hidler et al., 2009; Hornby et al., 2008). This may be due, in part, to the relatively smaller number of clinical studies but it may also be due to the fact that early lower-extremity therapy robots were designed to impose motion rather than provide guidance (Neckel et al., 2008; Israel et al., 2006). More recent designs for locomotor therapy have begun to address the formidable challenge of providing highly "back-drivable" (low impedance) interaction (Roy et al., 2009; Veneman et al., 2007) while supporting substantial fractions of body weight (Roberts, 2004).

Additional examples of high force haptic applications include human-assistive and exoskeletal devices (Guizzo & Goldstein, 2005, Kazerooni & Guo, 1993), physically cooperative man-machine systems (Peshkin et al., 2001) and similar applications. Like these

other high force haptic devices, successful therapy robots must simultaneously embody a formidable set of capabilities, usually including all of the following:

1) The capacity to deliver large forces, sufficient to move human limbs actively against strong muscular effort by the subject (e.g. due to abnormal tone), and in some cases (e.g. balance & locomotion) to support substantial fractions of body weight
2) The ability to represent controlled, virtual environments (e.g. virtual walls or springs), in order to provide physical guidance, assistance (but only as needed), protection from force spikes, resistance (e.g. for strength training), and to communicate information
3) The ability to be backdriven, to avoid inhibiting a patient or operator's attempts to move or observe the outcomes of these efforts
4) Large workspaces, up to a cubic meter or more, to accommodate the range of motion of human limbs
5) A number and arrangement of degrees of freedom compatible with large and small scale human movement
6) Guaranteed stability and safety while exchanging significant force and power with non-expert, impaired and unpredictable human subjects

In contrast, most existing haptic and robotic systems embody some subset of this list of features, but not all. More specifically, most existing robotic devices have either low force capacity with low mechanical impedance or high force capacity with high intrinsic impedance. Achieving this full set of features is a formidable engineering challenge that is limited by existing actuator and control technologies.

In this chapter we provide an overview of the tools available to address the high force haptic challenge by summarizing and critiquing available techniques, discussing several advanced approaches that show promise, and presenting a novel actuator architecture that may provide a superior solution for certain high force haptic applications. In the next section performance and stability considerations for high force haptic systems are summarized. Section 3 discusses the utility of available actuator and interaction control technologies for high force haptics. Section 4 introduces a novel hybrid actuator architecture that circumvents the fundamental limitations plaguing actuators for high force haptics. Analysis and experimental validation of a simple example are included. Concluding remarks are provided in Section 5. The prior and novel work presented here provides the foundation of a nascent toolkit of methods to design and build effective high force haptic machines.

2. Performance and Stability of High Force Haptic Systems

Haptic systems consist of a union between an engineered mechanical system (a haptic device) and a human operator. While haptic devices and robots both include actuators, sensors, control software, and mechanisms designed to achieve particular kinematics, haptics differ from most common robots because the physical coupling to an unknown and unpredictable human subject has a strong influence, by design, on the system's behavior. From a control standpoint, this significantly influences how both performance and stability are understood. For a traditional motion-controlled robotic system, performance is measured by the system's ability to track trajectories or move to locations in space. Stability is determined by the robot and its controller, possibly with consideration of static payloads.

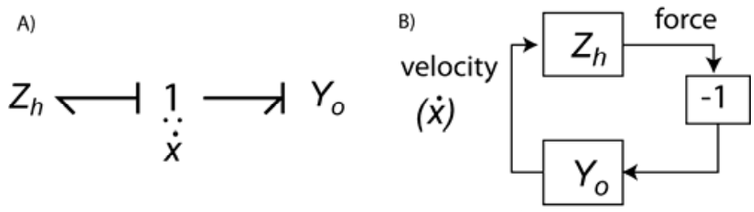

Fig. 1. Physical interaction between a haptic device and human operator, represented by port functions. A) Bond graph representation. B) Block diagram representation.

For haptic devices, the considerations are quite different. Rather than control motion, haptic devices are intended to represent virtual objects, meaning that they must convincingly transition between apparent free motion and apparent contact with objects with specified physical properties. Performance is best understood as the quality of the virtual environment, or the "feel" presented to the operator by the haptic device. Furthermore, the operator is a dynamic system that is physically coupled to the haptic device. A critical distinction between typical robots and haptic devices is as follows: In robotic systems, performance and stability are both properties of the robot. In haptic systems, including high force haptic systems, performance is solely a property of the haptic device, while stability depends on *both* the human operator and the haptic device. This indicates that traditional methods of analyzing the performance and stability of robotic systems are not ideally suited to analyzing high force haptic systems.

A proven method for analyzing physically coupled systems uses *port functions* to model energy flow between systems at physical points of interaction, or *power ports* (Hogan & Buerger, 2005). Port functions define the behavior of each system in terms of the relationship between conjugate "effort" and "flow" power variables, depending on causality. Impedance (Z) provides the effort output in response to a flow input, while admittance (Y) is the inverse. In the mechanical domain, force (or torque) is the effort variable while velocity (or angular velocity) is the flow variable. Figure 1 shows two interacting systems: a haptic system represented by its impedance (Z_h) and a human operator represented by its admittance (Y_o). In this representation, the direction of power flow is purely a matter of convention; it is depicted as positive into each system. No assumption is required regarding the magnitude of either the impedance or admittance port functions.

The performance of the haptic device can be derived from its port impedance, which can be loosely thought of as dynamic stiffness, can be linear or nonlinear, and includes stiffness, inertia, friction and other dynamic behaviors, e.g. modes of vibration. Specifically, the intended feel at the interface can be represented by some virtual environment, which can be quantified by some impedance function, which may be linear or nonlinear and may vary in space and time. Performance can then be quantified by measuring the difference between the target impedance (or the target virtual environment) and that achieved in hardware. Phenomena that may detract from this performance can include unwanted inertia, compliance, or friction as well as unhelpful or distracting vibrations. This is consistent with the definitions of "fidelity" found in the haptics literature. A related performance metric, "transparency," generally refers to only the quality of the haptic hardware and its ability to minimize or disguise parasitic dynamics that are not part of the software-generated virtual environment (Carignan & Cleary, 2000). Specific high force haptic applications may benefit

from differing performance metrics based on the port impedance. For instance, when port impedance is linear or can be approximated as such, performance can be defined as a cost function *C* that consists of a frequency-weighted integral of the difference between the magnitudes of the actual *(Z)* and target *(Z_{targ})* impedance functions (normalized to 1 Ns/m to make the argument of the log dimensionless), yielding a single number to minimize:

$$C = \int_{\omega_0}^{\omega_1} W(\omega)\left|\log\left|Z(j\omega)\right| - \log\left|Z_{targ}(j\omega)\right|\right| d\omega \tag{1}$$

The weighting function *W* can be used to emphasize general frequency regions of interest or particular features such as precise resonances, and ω can be replaced with its log to achieve logarithmic frequency weighting. In other cases more insight may be gained by quantifying performance in terms of intuitively familiar physical quantities such as the apparent inertia, Coulomb friction, etc. Metrics may be more complex when the port impedance is nonlinear, and performance can also be measured in the time domain, based on the desired and actual response to particular excitation at the port. Regardless of the specific metric used, we contend that performance of a high force haptic system derives from the port behavior as quantified by the mechanical impedance.

In contrast, the stability of an interactive system like that shown in figure 1 depends on the dynamic properties of both coupled ports. If both port functions are linear, the characteristic polynomial of the system in Fig. 1B is

$$1+Z_h Y_o. \tag{2}$$

The stability of the coupled system, termed *coupled stability* (Colgate & Hogan, 1988), is determined by the real part of the roots of this quantity. Clearly, the dynamics of the human operator contribute fundamentally to total system stability. This fact, taken with the previous paragraph, highlights an important distinction between physically interactive systems and servo controlled systems. In linear servo controlled systems, the same characteristic equation determines closed-loop stability and influences performance (in terms of frequency response, time response, etc.) In linear interactive systems, performance is dictated by the port function of the haptic system alone (Z_h) while stability is determined by equation 2, which includes properties of the operator as well (Buerger & Hogan, 2007).

Because the dynamic properties of the operator cannot be controlled by the haptic system designer, guaranteeing coupled stability poses a challenge. One valuable concept for understanding coupled system stability is *passivity*. A power port with a passive port function cannot release more energy than has been put into it. For the linear time-invariant case, a system defined by the linear 1-port impedance function $Z_p(s)$ is passive iff:

1. $Z_p(s)$ has no poles in the right half plane
2. Any imaginary poles of $Z_p(s)$ are simple, and have positive real residues
3. $Re(Z_p(j\omega)) \geq 0$ (3)

Such a port function has phase between -90° and +90° for all frequencies. Colgate showed that when two passive port functions are coupled together as in Fig. 1, the total open-loop phase must be between -180° and +180° at all frequencies, and the Nyquist stability criterion cannot be violated, so the coupled pair is guaranteed to be stable (Colgate & Hogan, 1988).

This is consistent with the energy properties of passive ports. If two passive ports are coupled, neither can generate energy indefinitely, and therefore stability is guaranteed. Because it is energy based, this extraordinarily powerful result works for linear and nonlinear systems (for nonlinear extensions, see e.g. (Wyatt et al., 1981)), and applies (perhaps with fine tuning) to all physical domains. To the extent that humans can be assumed to act as passive mechanical systems at their ports of interaction, passivity provides a powerful stability metric for high force haptics. While this has not been conclusively proven, given the complexities of the neuromuscular system, available empirical results and theory strongly suggest that this is indeed the case (Hogan, 1989). Unfortunately, making high force haptic systems passive can often limit performance. Certain simple control laws can preserve passivity, but given the limitations of available actuator hardware, these simple controllers often can not achieve adequate performance at the haptic system port. These challenges are reviewed in the next section.

3. Actuator and Control Technology for High Force Haptic Systems

Ideal high force haptic systems would achieve high forces while representing port impedance ranging from near zero to near infinite stiffness, friction and inertia, while guaranteeing passivity and coupled stability. Actuators for these idealized systems would require similar properties, plus some additional properties (e.g. low mass), depending on the system configuration. In this section we assess the value of various technologies in approaching this ideal, first by seeking a purely physical solution in the form of actuators effective at human scales (tens to hundreds of N, cm to m motions, frequencies less than 10 Hz), then by exploring the benefits of available advanced control methods.

3.1 Classical Actuator Technologies for High Force Haptics

Electromagnetic actuators can represent desired forces with extremely high fidelity when used in direct drive configurations. Friction can be extraordinarily low, especially at the low frequencies typical of interaction with humans (at higher frequencies eddy current or IR losses create drag). With the low intrinsic impedance of these actuators, simple and robust control algorithms, discussed below, may be used to provide a stiff interface and to preserve passivity. The main drawback is limited force density (Hollerbach et al., 1992), meaning that high forces lead to large, heavy actuators. Electromagnetic actuators are easy to use, and in many cases systems can be successfully designed to meet certain limited requirements in spite of force density limitations. An example is the MIT-MANUS robot for upper-limb physical therapy, which uses direct-drive rotary motors with a two-DOF (degree of freedom) planar closed-chain configuration that allows both actuators to remain stationary (Krebs et al., 2004). Other devices are effective due to very small translational workspaces (Berkelman et al., 1996). The force density limitation is far more difficult to overcome for open-chain serial systems. If the actuator for DOF #1 is carried by DOF #2, as is common for serial robot arms, then the mass of the actuator not only increases the force required for the DOF #2 actuator, but also adds to the endpoint inertia of that DOF. This problem emerges for most non-planar mechanisms, and is therefore very common. As forces increase, carrying the full weight of direct drive actuators rapidly becomes prohibitive. When rotary motors cannot be used, large motions pose an additional problem, as the high mass per unit force increases nearly linearly with range of motion.

An obvious way to improve the force density of electromagnetic or other actuators is to add gearing. This approach makes carrying actuators in a serial mechanism feasible and is used extensively in robots. Unfortunately a gear train compromises endpoint impedance, increasing the actuator's apparent inertia and friction due to eddy current or IR losses, as observed at the endpoint, by the square of the gear ratio. Coulomb friction and stiction in the actuator are amplified linearly by the gear ratio. Furthermore, the gear train adds its own friction, inertia and backlash. As a result, even when transmissions are designed explicitly to minimize friction, high impedance is difficult to escape (Buerger et al., 2001). While some applications are amenable to modest gear ratios (typically less than about 5:1), larger gear ratios rapidly lead to unacceptable levels of reflected inertia and friction. The failure of gearing to solve the underlying force density problem in high force haptics distinguishes this problem from most robotics, where gearing is generally very successful.

The most significant problem with using direct-drive electromagnetic actuators for high force haptics is the need to carry their substantial mass when complex or serial mechanisms are used. Mechanical transmissions such as cables, belts, tapes and rods offer a potential opportunity to keep the actuators stationary or nearly stationary, in some robot configurations, while transmitting their force, motion and impedance properties to the interaction port. Cable transmissions, in particular, have been elegantly and cleverly designed to achieve reasonable force and impedance capabilities in high-DOF serial arms, e.g. the WAM arm (Townsend & Guertin, 1999). The complexity of the mechanisms that enable the WAM underscore the fact that routing of mechanical transmission members can be extremely challenging. When actuators for multiple DOFs of a serial mechanism are mounted at the base, the transmission elements for one or more DOFs must pass through or around other joint(s). This presents an extreme packaging challenge as the number of DOFs grows, and this challenge is compounded by the fact that fixed separation must generally be maintained between transmission nodes (e.g. between pulleys in a cable system). Cables, belts and transmission tapes must be held in tension, requiring tight, deterministic coupling between the actuators and the intermediate and terminal joints that they actuate, even as the intermediate joints are independently actuated. These flexible members also tend to introduce problematic dynamic resonances (a "guitar-string" effect) and can severely limit bandwidth. Transmission rods can be made more rigid, but present an even more difficult plumbing challenge, as the gears that mate adjacent rods must be kept in tightly controlled contact. In certain configurations, mechanical transmissions can offer an acceptable high force haptic solution, and thus represent an important tool. However, for other applications their limitations are insurmountable, and other options must be sought.

Appealingly, hydraulic actuators can achieve force densities at least an order of magnitude better than ungeared electromagnetic motors (Hollerbach et al., 1992). Because the working fluid is nominally incompressible, hydraulics can achieve very high stiffness relative to humans. Pressure sources and valves can be located remotely, with force and motion coupled to the interaction port through flexible tubing, which can be routed with greater flexibility than mechanical transmission elements. In spite of these apparent advantages hydraulics have been little-used for haptic interfaces (with some exceptions, e.g. see (Kazerooni & Guo, 1993, Lee & Ryu, 2008)). This is because the operation of conventional servovalves causes hydraulic actuators to have high intrinsic impedance, and in fact generally to be non-backdrivable. Hydraulic actuators rely on nonzero valve impedance to

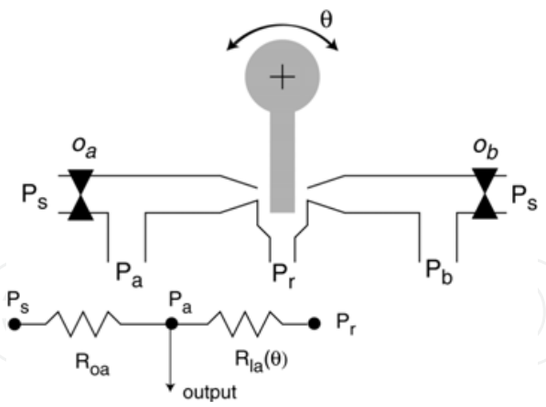

Fig. 2. Schematic of flapper servovalve, with resistor model of left half.

regulate output, placing a lower limit on the output impedance. The fundamental nature of this limit can be demonstrated by considering a typical pressure control valve design.

A servohydraulic system includes a high-pressure energy source, usually controlled to produce nominally constant pressure P_s, and a servovalve connected to a control system that meters the flow (or pressure, depending on the valve design and control structure) to the actuator, where energy is converted to mechanical energy. The servovalve determines the mechanical characteristics of the output, including force or motion as well as the mechanical impedance. A common valve architecture for pressure regulation is the flapper valve, shown schematically in Fig. 2 (jet-pipes offer a different configuration subject to largely similar tradeoffs). The flapper configuration is used, for example, as the first stage of the Moog Series 15 pressure control valves (www.moog.com). The output of this valve is the differential pressure (P_a-P_b). Two streams of fluid from the high-pressure source P_s push in opposite directions against the flapper, which is attached to the rotor. Both fluid streams then drip to the return at pressure P_r. The flapper rotates to partially restrict one side and raise the fluid pressure in that branch. For the change in fluid resistance at the flapper to have an impact on P_a and P_b, each side of the valve must be separated from P_s by an orifice (o_a and o_b). Unfortunately, any fluid supplied to the load must pass through one of these orifices, increasing the impedance and degrading the valve's quality as a pressure source.

This can be seen if the left half of the valve is modeled as a pair of fluid resistors, as shown below the schematic. The input orifice is modeled as the resistor R_{oa}, and the flapper opening is modeled as the resistor $R_{la}(\theta)$, which creates a pressure drop between P_a and the return pressure P_r and depends on the rotor angular position θ. If $R_{oa}=0$, then the output pressure $P_a = P_s$, and the actuated flapper has no effect on output. If a single fixed rotor position $\theta=\theta_o$ is considered, $R_{la}=R_{la}(\theta_o)$. Deriving the output impedance $Z_a = P_a / Q_a$, where Q_a is the volumetric output flow rate, produces:

$$Z_a = \frac{R_{oa} R_{la}}{R_{oa} + R_{la}} \tag{4}$$

A pure pressure source would have $Z_a=0$. If R_{oa} is too small, then changes in $R_{la}(\theta)$ have little effect on the output pressure P_a, and the valve will not function. Z_a can be made small by minimizing R_{la}. However, the total valve output impedance is:

$$Z = Z_a + Z_b \tag{5}$$

where Z_b is the port impedance for the other side of the valve, and has the same form as Eq. (4). But $R_{lb}(\theta)$ increases when $R_{la}(\theta)$ decreases, so the only way for the total output impedance to be low is for both flapper resistances to be low. This would allow substantial leakage through the flapper and would significantly reduce the output pressure. To achieve high output pressure requires amplification in a second stage (as in the Moog series 15 valve). The problems with this amplifier are twofold: first, even if it operates perfectly, it amplifies the impedance of the first stage at the endpoint by acting as a gear mechanism (hydraulic gearing is analogous to mechanical gearing); and second, it introduces more small orifices through which the fluid must flow. Enlarging the orifices in both valve stages simply produces a leaky valve, increasing power consumption and reducing efficiency. Thus without pressure feedback, the only way to avoid high impedance is with substantial leakage flow, which increases compressor size. Given the stringent impedance requirements of high force haptics, the leaky valve approach is generally impractical. High impedance in the valve is directly related to the ability generate output pressure, and cannot be eliminated. Furthermore, sliding cylinder seals represent another source of unwanted friction that can be challenging to avoid, particularly if operating at high pressures. Narrow pressure lines also contribute viscous damping and inertia. Another disadvantage of hydraulics is that at high pressures, safety risks can arise if lines rupture; however, the modest forces (by hydraulic standards) required for human interaction mitigate this hazard. Finally, the compressors needed for servohydraulic systems are usually heavy and noisy and therefore problematic for close proximity to human subjects. In section 4 of this chapter, we argue that in spite of these limitations, the force density advantage of hydraulics warrants further consideration in different configurations for high force haptics, and we present an architecture that circumvents the high-impedance servovalve challenge.

Pneumatic actuators are also capable of high force densities (Hollerbach et al., 1992) and provide behaviors unique among actuator technologies. While regulators that control gas pressure rely on flow restriction, much like hydraulic servovalves, low impedance is readily achieved due to the compressibility of the working fluid. Indeed gas compressibility presents one avenue to modulate the endpoint impedance, by directly manipulating the properties of the enclosed volume of gas in the actuator. However, representing high stiffness requires high pressure, and transitioning from low to high stiffness (e.g. to represent a virtual wall) requires rapid pressure changes. This can be understood by considering the simple example of a closed cylinder in compression due to force from a piston with cross-sectional area A, shown in Fig. 3. For simplicity isothermal conditions are assumed. Adiabatic conditions yield similar conclusions. Behavior at the port of interaction with the operator is characterized by the applied force F and displacement x. The gas in the cylinder is at the absolute pressure P, and the specific gas constant R and temperature T are fixed, while the volume V varies with x. P_{amb} denotes ambient pressure. A mass m of an ideal gas with molar mass M, is contained in the cylinder. The ideal gas law for this volume is:

$$PV = \frac{m}{M}RT \tag{6}$$

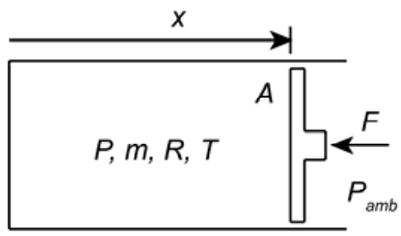

Fig. 3. Schematic of an ideal gas under isothermal compression in a piston-cylinder.

Pressure consists of ambient plus that due to the applied force:

$$P = \frac{F}{A} + P_{amb} \tag{7}$$

Substituting $V=Ax$ and eq. (7) into eq. (6) and rearranging produces:

$$F = \frac{RT}{M}\frac{m}{x} - P_{amb}A \tag{8}$$

Differentiating produces the stiffness:

$$\frac{dF}{dx} = -\frac{RT}{M}\frac{m}{x^2} \tag{9}$$

For fixed (or nearly fixed) x, for example when traversing a virtual wall, stiffness is proportional to the enclosed mass. To simulate a virtual wall with stiffness 100 times greater inside the wall than out purely by manipulating the properties of the enclosed fluid requires increasing the enclosed mass by a factor of 100 within the period of simulated contact with the wall. From eq. (6), this means that the pressure also must increase 100-fold. (For a real implementation, something must also offset the force due to increased pressure, usually a pressure against the other face of the piston). Thus discrete virtual environment features such as virtual walls are extremely difficult and inefficient to implement in this way. Another problem shown by eq. (9) is that stiffness is highly nonlinear in x, meaning the pressure must also be varied to maintain linear stiffness, if that is desired. An alternative approach would be to always operate at high pressures, keeping the transmission stiff, and modulating impedance at the valve source. Unfortunately this presents the same high intrinsic impedance challenge described in detail above for hydraulics. Pneumatic actuators are notoriously difficult to control, and the additional challenges of high force haptics exacerbate the problems. The fluid dynamics of pneumatic actuators are also forbidding for implementing closed-loop control using a regulator to respond to measured endpoint forces. Venting can be used to eliminate resistance from the gas, but this can be quite inefficient. Finally, compressed gas stores orders of magnitude more energy than liquids at the same pressures, and this can raise potential safety concerns. In spite of their challenges, pneumatic actuators have been proposed for certain haptic and high force haptic applications where their intrinsic compliance can be beneficial, including exoskeletal devices (Tressler et al., 2002) and other devices employing pneumatic muscles (Tondu & Lopez, 2000).

3.2 Interaction Control

Physical interaction requires control strategies that differ significantly from the more common position or velocity servo problems. Because of the unique characteristics of physical interaction described above, the prevailing approach is explicitly to regulate dynamic behavior at the port(s) of interaction, e.g. by using *impedance control* (Hogan, 1985). The most straightforward embodiment of this theory, termed simple impedance control, uses motion feedback with torque- or force-producing actuators to implement virtual dynamics on low-impedance hardware. Proportional position feedback produces virtual stiffness, and proportional velocity feedback (or derivative position feedback) produces virtual viscous damping. If implemented ideally with positive gains and co-located sensors and actuators, the result is passive port impedance (Hogan & Buerger, 2005). This approach is powerful, robust and easily implemented, and has been applied successfully (Krebs et al., 2004). Its major limitation is the need for low-impedance hardware. Simple impedance control can do nothing to counteract inertia and friction in the physical system. Thus while simple impedance control can effectively stabilize interaction by guaranteeing passivity, it can do little to address the limitations of actuator technology discussed in the previous section, providing significant motivation for the alternative techniques discussed here.

A class of control methods has been developed that uses measured forces (torques) at the port of interaction to close a feedback loop and expand the range of apparent dynamics that can be presented. This approach has the potential to mask the physical properties of the hardware, presenting a desired dynamic response at the port of interaction that closely tracks target dynamics derived independent of the physical hardware. For instance, the apparent inertia and friction can be reduced below the physical values by using the actuators to drive the device in the direction of applied force. When the target impedance is zero, this is termed force control. Unfortunately this approach seriously threatens coupled stability; in fact passivity is lost whenever the apparent inertia is reduced by more than a factor of two below the physical inertia (Colgate & Hogan, 1988, Newman, 1992). Natural admittance control exploits the fact that loss of passivity derives from reducing the apparent inertia, rather than the friction. This method provides a means of theoretically ensuring passivity while aggressively reducing the apparent friction well below the physical level by keeping the inertia at a level that ensures passivity (Newman, 1992). This approach can dramatically improve feel by virtually eliminating static friction, but cannot mitigate high levels of physical inertia, which are particularly common in geared actuator systems.

An alternative approach recognizes that passivity, though sufficient to stabilize interaction with human subjects, is not necessary. Passivity ensures stability when coupled to a wide range of environments including large inertial loads, kinematic constraints, highly nonlinear frictional contact, etc. On the other hand, the dynamic characteristics of human limbs are considerably more limited, even as they vary in time, configuration and across subjects. Port stability can be posited as a robust stability problem with conservative bounding values used for operator dynamic properties, and robust control methods can be used to shape the dynamics of the force feedback control loop to maximize performance (by minimizing impedance error) while guaranteeing coupled stability (Buerger & Hogan, 2007).

3.3 Advanced actuators

In spite of significant progress in advanced interaction control, achieving all six required characteristics of high force haptic devices listed in section 1 remains a persistent challenge, particularly for complex and high-DOF devices. Several recent advances in actuator development offer promising future alternatives for the high force haptic designer's toolbox.

Goldfarb has described monopropellant-powered actuators that chemically generate gas to produce pressure, and force output (Goldfarb et al., 2003). This approach dramatically improves energy density and eliminates the need for a compressor. However, force and impedance properties—and limitations—appear to be fundamentally similar to those of compressed-air systems. In particular, rapid changes of stiffness (to simulate contacting a surface) require high mass flow rates. Dramatic thermal changes would also impact endpoint impedance. In the authors' opinion, this approach seems quite promising, though as yet unproven for high force haptics.

Series elastic actuators, which include compliant members placed between high-impedance source actuators and the environment and use force feedback control, can achieve high force-density and low impedance (Pratt & Williamson, 1995). The elastic element provides several advantages for certain applications, but does not guarantee passivity, and a careful tuning process is generally required to achieve stability. This is problematic when interacting with variable, unpredictable humans. An alternative design method that includes carefully controlled physical damping in conjunction with natural admittance control can theoretically guarantee passivity (Dohring & Newman, 2002). Generally, the more aggressive the reduction of apparent impedance from the physical actuator level, the softer the compliant element must be. This limits the utility of this approach by limiting achievable stiffness. Still, carefully designed series dynamics are an important tool.

Research into electroactive and dielectric polymers has shown potential for high achievable stresses. These muscle-like materials could one day produce effective high force haptic actuators, but have not yet been shown to scale up to the forces needed (Bar-Cohen, 2004).

To the best of our knowledge, no existing actuator technology or control strategy provides a comprehensive solution for high force haptics. Additional tools are needed to improve the tradeoffs between force capacity, DOFs, workspace size, interface fidelity, and coupled stability. An alternative way of evaluating the potential of major human-scale actuator technologies is by available stress, which is strongly related to force density. The force output of electromagnetic actuators is limited by the shear stress in the air gap between moving and stationary components, which is typically tens of pounds per square inch (psi). Pneumatic actuators can achieve hundreds of psi but rapidly introduce hazards as pressure is elevated, due to high levels of stored energy. By contrast, hydraulic actuators routinely achieve thousands of psi (McBean & Breazeal, 2004). This fundamental promise warrants a second look at hydraulics to see if the underlying high impedance of servovalves can be avoided, and if the tradeoffs between the six criteria listed in section 1 can be improved.

4. Hybrid hydraulic actuators for high force haptics

Among actuator technologies available at the human scale, hydraulic actuators are alone in offering high force density, high stiffness, and flexible connectivity between power sources and the interaction port. Their main drawback is high impedance, which derives primarily from servovalves, and because of this they have been little-used for haptic interfaces. By contrast, electromagnetic actuators are widely used for haptics due to their favorable force and impedance behavior, but suffer from dramatically inferior force density. A hydraulic actuator capable of controlling pressure with low impedance rather than a high impedance servovalve would be a powerful development. We have investigated a hybrid architecture for actuators that exploits the benefits of both hydraulic and electromagnetic actuation while circumventing the weaknesses of each. In this design, sketched in Fig. 4, a hydraulic element is used purely as a transmission, while a remotely-located source actuator provides force and motion, and dictates the representation of the virtual environment. The hydraulic transmission is stiff in the direction of actuation but is embodied in flexible tubing, such that motion of the interaction port is decoupled from motion of the source actuator, and the source actuator may remain stationary. Critically, this architecture obviates the need for a hydraulic servovalve, eliminating the main cause of high impedance. The hydraulic transmission is analogous to a mechanical transmission but, unlike cables, tapes or rods, does not require a deterministic coupling between source and interaction port locations. This architecture also enables the use of effective source actuators, particularly direct-drive electromagnetic actuators, that can provide favorable force, motion and impedance properties. The source actuator can have large mass, because it need not move.

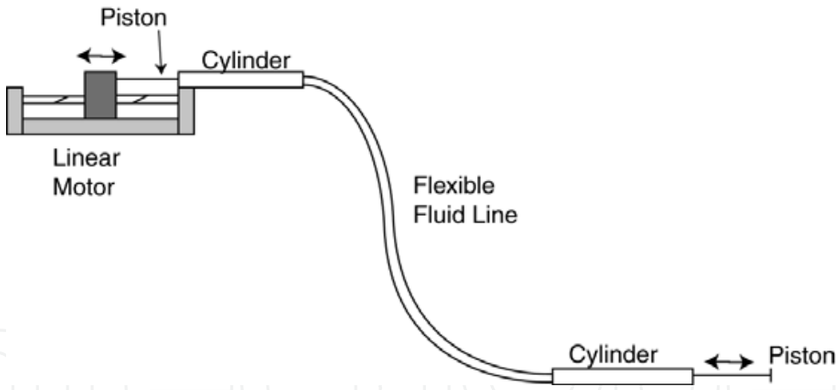

Fig. 4. Schematic of linear actuation scheme with fluid transmission.

While this proposed architecture can dramatically reduce endpoint mass, in its simplest form it actually increases the total system mass when compared to using only direct drive electromagnetic actuators. (The hydraulic transmission would be unnecessary if the actuator was connected directly to the endpoint.) Total mass is critically important for some applications (e.g. fully mobile exoskeletons), and this approach may not be suitable for those. However, in many cases the *placement* of mass is of equal or greater importance than total mass. Therapeutic robots, for instance, may tolerate being tethered to a stationary or independently mobile collection of heavy components, e.g. for power (Roberts, 2004). On the other hand, the absence of a compressor may lead to a lower system mass than a pure

hydraulic system. This passive hydraulic architecture decouples a portion of the drivetrain from the mobile interaction port and conducts energy to it in hydraulic, not electrical, form.

4.1 Design Model and Tradeoffs

Figure 4 shows a schematic of one embodiment of this architecture that uses a linear electromagnetic motor as a source actuator and a passive hydraulic system as a power transmission. The hydraulic system consists of a piston/cylinder on each end for conversion between mechanical and fluid power, and a flexible hose connecting the two. One piston connects to the source motor, and the other acts as an actuator. Unlike servovalve-controlled hydraulics, the mechanical piston-cylinders, each of which acts as both an energy and signal source for the hydraulics, and the tubing that joins them need not include small orifices to regulate pressure, and can be designed to have relatively low intrinsic impedance.

If the source actuator is capable of providing the desired force and impedance, then an ideal transmission is mechanically *transparent*. In this context, transparency (previously used to describe an objective for bilateral teleoperation systems (Lawrence, 1993)) means that the force, motion, and energy exchanged between a load and the transmission is equal to that exchanged between the transmission and the source actuator. The goal is to transport actuator behavior to a remote endpoint package that weighs less than the source. Figure 5 depicts a generic transmission architecture. If the transmission is perfectly transparent, the motion trajectories of ports 1 and 2 are identical for all time, the force exchanged at port 2 equals that exchanged at port 1, and the impedance at the interface to the environment exactly equals the actuator impedance. That is, a perfectly transparent transmission is lossless and has the following properties:

$$\begin{aligned} x_2(t) &= x_1(t) \\ F_2(t) &= F_1(t) \\ Z_p &= Z_r \end{aligned} \tag{10}$$

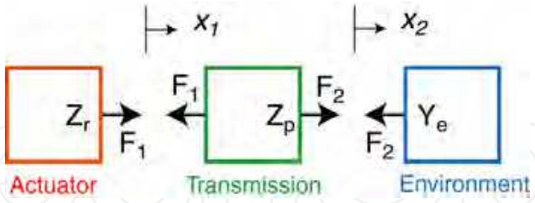

Fig. 5. Schematic depiction of a transmission between a source actuator and environment.

Any practical transmission will drain some energy and will therefore not be perfectly transparent. Furthermore any real physical system has nonzero inertial and compliant dynamics. To approach ideal behavior, the transmission should be designed to minimize inertia, compliance, and friction (although transmission dynamics may be used to advantageously shape the port impedance; see 4.3). While transparency is an important performance objective, an effective transmission must also be *flexible*. A perfectly flexible transmission would allow infinite separation (in all spatial degrees of freedom) of the endpoint package from the source actuator with zero reaction forces (torques). A practical transmission must provide sufficient freedom of motion from the source to cover the robot's

workspace. Forces and torques required to bend and twist the fluid line should be minimized. The requirements of flexibility and transparency are often in conflict, as detailed below. Whether a transmission is intended to be transparent or to shape impedance, its design specifications focus on how it impacts endpoint impedance. This distinguishes high-force haptic applications from conventional servo problems. Below we provide a model that enables the prediction of the transmission's transparency and its impact on endpoint impedance. First several issues must be addressed to ensure that useful actuators capable of bilateral power transmission can be configured and controlled to operate as intended.

From Figure 4 it is straightforward to envision the hydraulic components transmitting force, motion and power in compression. However most high force haptic systems must sometimes actuate bilaterally (pulling as well as pushing). If tensile forces are applied to a closed liquid volume, its pressure drops below ambient and the fluid evaporates locally (cavitates). If the seals are imperfect, air leaks in. Two simple options enable bilateral actuation: a bias pressure that exceeds the pressure needed to transmit tensile forces can be introduced, or actuator pairs can be used together. The latter is depicted in Figure 6, wherein the two actuation paths exist within the same two cylinders, joined by two separate fluid lines, one for "tension" and the other for "compression." This configuration introduces several difficulties, including additional weight and complexity as well as additional seals. Seals where the pistons exit the cylinders are particularly problematic, as any liquid that leaks there leaves the constant-volume system and must be replaced.

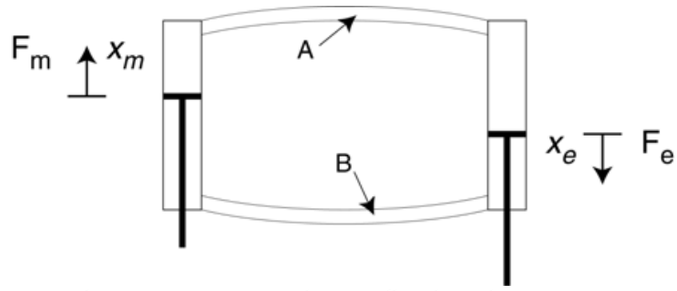

Fig. 6. Bilaterally actuated transmission with two fluid paths.

A simpler method of tensile force transmission that uses a single fluid path requires mechanically creating a bias pressure such that the fluid pressure is elevated **a**bove ambient without force applied by the actuator or environment. This can be accomplished by applying a constant compressive force to each piston. When the system is at rest, the forces on each side cancel, but the fluid in the chamber is at an elevated pressure. Tensile forces reduce the pressure, but if the force does not exceed the bias force level, the fluid pressure remains above ambient and cavitation and gas leakage into the system are avoided. This approach requires additional hardware to create the applied load, and increases the operating fluid pressure, but requires only two moving seals rather than four.

Using this mechanical bias force approach, the transmission can be modeled for design purposes as the simple straight-pipe system shown in Fig. 7. This model, used as the design basis for determining transmission impedance, includes each of the piston-cylinders (with diameters D_1 and D_2 and length L_1) and approximates the flexible line that connects them as

a straight, smooth and rigid cylindrical pipe (with diameter D and length L). The forces applied to the two pistons are F_1 and F_2, and the piston velocities are v_1 and v_2. The bulk fluid velocity in the line is v. The transition from piston diameter to hose diameter must also be considered. This simplified model can be used to predict losses due to friction, the weight of the fluid in the system, and the inertia due to fluid acceleration. Calculations based on this particular model are summarized below to illustrate the relationship between transmission geometry and system performance. From Fig. 7 it is evident that this hydraulic transmission can also provide an intrinsic gear reduction for force (or motion) amplification or reduction, without adding mechanical parts that might contribute backlash or friction. In this case, the gear ratio is equal to the ratio of the piston areas.

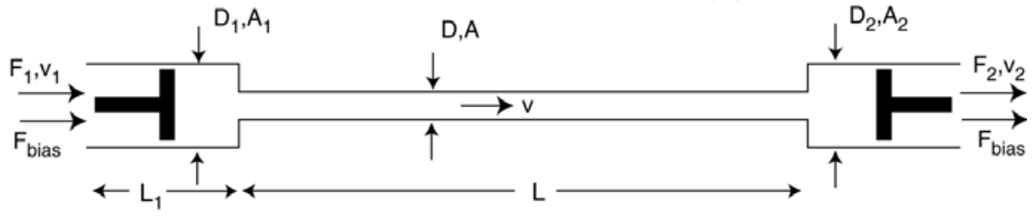

Fig. 7. Straight-pipe, dual piston model for a linear passive hydraulic transmission.

To be viable, the proposed actuator architecture must be amenable to control. By introducing a significant separation between the source actuator and the endpoint where behavior is controlled, with accompanying transmission dynamics, the structure of the system poses a potential challenge for effective and highly stable control. Because stability and passivity are paramount, one way to represent target impedance is to feed back motion only at the source actuator, closing a simple impedance control loop around only the well-characterized electromagnetic source actuator, yielding a robustly stable implementation. This arrangement depends on the transmission to reliably (and nearly transparently) transmit impedance between the source actuator and operator, but without using a sensor at the interaction port, it may be vulnerable to small and accumulating position errors. Fortunately, although humans excel at gathering information from physical contact, they are not generally sensitive to small changes in position. Provided that physical contact is represented as intended, small positioning errors can be tolerated with very little consequence, especially if the device is used in conjunction with a visual display. Compared to alternative transmission implementations (e.g. cable drives), a hydraulic transmission may provide superior damping of resonant transmission line modes via the intrinsic viscous behavior of the working fluid, and in fact the dynamics of the transmission may be intentionally sculpted to improve both interaction stability and performance via *impedance shaping*, as discussed briefly below.

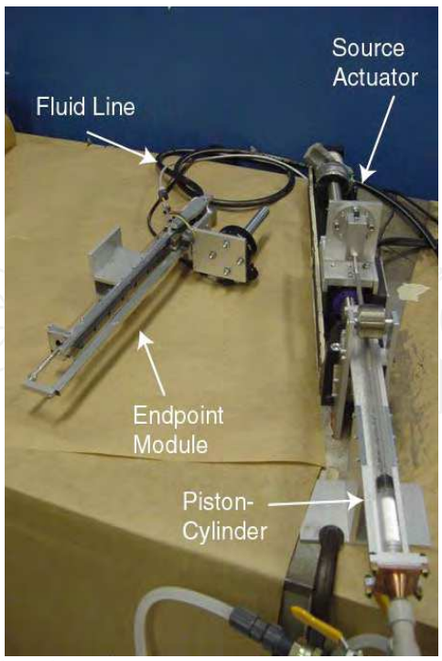

Fig. 8. Prototype passive hydraulic transmission system with linear source actuator.

To illustrate the key design issues for this architecture, a representative design problem is presented by applying the model in Fig. 7 to the specifications for an actuator for an upper-limb physical therapy robot device. This is intended as an out-of-plane "anti-gravity" addition to the planar MIT-MANUS robot, and has previously been addressed with two designs, one using a rotary electric motor and a low-friction roller screw and the other a direct-drive linear electromagnetic motor (Buerger et al., 2001, Krebs et al., 2004). The stringent and challenging target specifications for this application include a range of motion of 0.4 m, a force capacity of at least 65 N, a mass of less than 2 kg at the endpoint, a separation of at least 3 m between the stationary source actuator and the mobile endpoint, achievable stiffness of at least 2 kN/m, and minimal endpoint impedance including inertia less than 2 kg, Coulomb friction less than 2 N, and linear damping coefficient of no more than 10 Ns/m. Both previous designs violated the mass specification by nearly a factor of four. In this section the design model is developed to predict frictional and inertial dynamics of the transmission, and compliance is discussed. A prototype actuator (Fig. 8) was fabricated and its measured properties are discussed in the next section.

Damping: A major advantage of this configuration is its ability to avoid or minimize the viscous losses that arise in conventional hydraulics from forcing large volumes of fluid through small control orifices. Nevertheless, the long, narrow transmission line contributes some damping due to viscous drag. Assuming the fluid in Fig. 7 is incompressible, steady flow between any two points in the pipe is governed by the following expression, derived from the energy equation:

$$\left(\frac{P_1}{\rho}+\alpha_1\frac{v_1^2}{2}+gz_1\right)-\left(\frac{P_2}{\rho}+\alpha_2\frac{v_2^2}{2}+gz_2\right)=h_{lt} \tag{11}$$

P_1 and P_2 are the pressures at each point in the pipe. ρ is the fluid density, α_1 and α_2 are kinetic energy coefficients related to the flow profile, z_1 and z_2 represent elevation, and g is the acceleration due to gravity. h_{lt} is the total head loss, representing the energy (per unit mass) lost between the two points. Selecting the two pistons as points 1 and 2, with equal cross-sectional areas, bulk velocities, and flow profiles, with no net change in elevation and a force F_1 applied to piston 1 but no force applied to piston 2, eq. (11) reduces to:

$$F_1 = A_1 \rho h_{lt} \tag{12}$$

which also uses the relationship:

$$P_1 = \frac{F_1}{A_1} \tag{13}$$

The head loss h_{lt} results from major losses due to the main fluid line body in addition to minor losses due to the changes in pipe area. The prototype was designed with tapered cylinder ends to restrict the minor losses to less than 5% of the major losses, so only the major losses need be considered. Major loss can be computed for laminar and turbulent flow with separate calculations, where turbulence depends on the piston velocities. For laminar flow (with Reynolds number less than 2300), the effective damping seen at the piston is linear with velocity and with the fluid viscosity μ, and is governed by the expression:

$$F_1 = 8\pi\mu L \left(\frac{D_1}{D}\right)^4 v_1 \tag{14}$$

The major damping at the piston is proportional to the *fourth power* of the ratio of piston diameter to pipe diameter (or the square of the area ratio A_1 / A). In other words, decreasing the pipe diameter increases damping dramatically in the laminar region. The same can be said of the turbulent region, where the Blasius equation can be used to predict losses when the Reynolds numbers exceeds 4000. The resulting expression is:

$$F_1 = \frac{\pi}{8} 0.3164 \mu^{0.25} \rho^{0.75} L \frac{D_1^{5.5}}{D^{4.75}} v_1^{1.75} \tag{15}$$

Turbulent damping is nonlinear in velocity, and even more highly dependent on the piston and line diameters.

Given the specification of a 3 m flexible line for the representative prototype, a design figure depicting the predicted friction versus velocity for several different hose diameters is shown in Fig. 9. A specification of a maximum of 10 Ns/m damping is also shown. Because the overwhelming majority of human patient subjects never exceed 0.4 m/s hand speed in the course of therapy, a hose with an inner diameter of 5/16" (0.79 cm) was selected for the prototype as it satisfies the design requirement for all relevant speeds. This hose has an outer diameter of approximately ½" (1.27 cm), and is comparable in size and flexibility to the electrical power cables that drive the source motor.

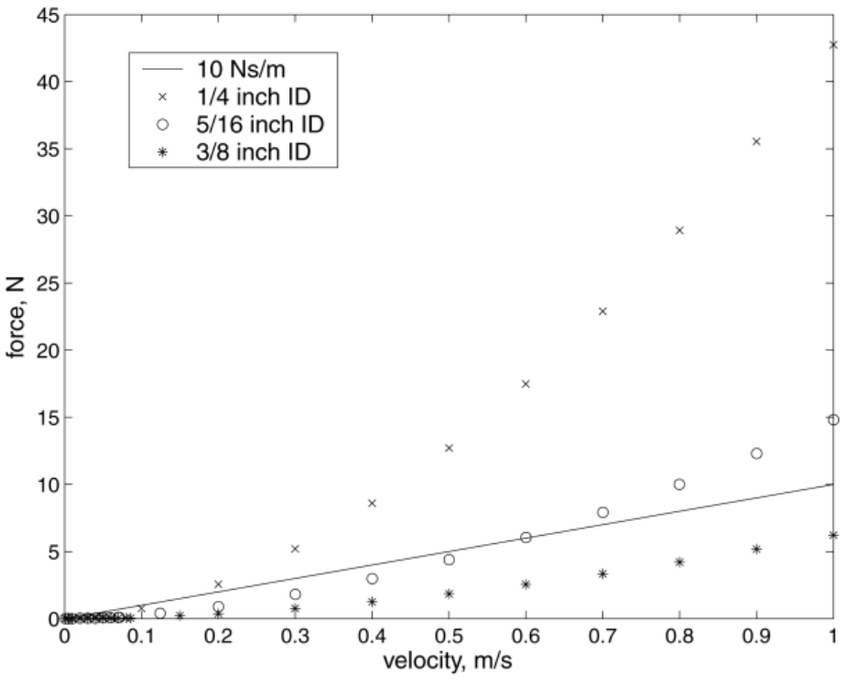

Fig. 9. Predicted fluid friction versus piston velocity, several hose diameters.

Inertia: The apparent endpoint inertia of the fluid transmission is another important factor that can be predicted from the Fig. 7 design model. Assuming incompressibility, the apparent mass m_{eq} at piston 1 can be determined from the total kinetic energy of the fluid:

$$m_{eq}\frac{v_1^2}{2} = m_{cyl}\frac{v_1^2}{2} + m_{line}\frac{v^2}{2} \tag{16}$$

m_{cyl} is the mass of the fluid in the two cylinders, while m_{line} is the mass of the fluid in the hose. Computation of m_{cyl} and m_{line} is straightforward from the density and system geometry but to determine m_{eq} the following relationship must be used:

$$v = \frac{A_1}{A}v_1 \tag{17}$$

The resulting equivalent inertia is:

$$m_{eq} = \rho L_1 \pi \frac{D_1^2}{4} + \rho L \pi \frac{D_1^4}{4D^2} \tag{18}$$

When the fluid line is long or narrow, the second term dominates. Decreasing the piston diameter D_1 decreases the system inertia but decreasing the line diameter D increases the inertia dramatically despite the fact that a smaller volume of fluid is used. This is because the fluid in the smaller line must accelerate much more rapidly, more than compensating for the fact that there is less of it.

Compliance: Assuming that the working fluid is incompressible and that air can be effectively eliminated from the transmission system, compliance can still result from the radial flexibility of the hose. Flexibility of the hose in bending is a direct performance requirement, and it is nearly impossible to create a tube that is very flexible in bending but very stiff radially. Designs that use radial reinforcements (for example braided fibers) to maximize the anisotropy of the hose are reasonably effective, but some radial compliance is unavoidable. This results in a fluid volume that expands as the pressure increases, changing the relative position of the two pistons. To maximize transparency, compliance should be minimized. Although hose anisotropy makes it difficult to predict compliance exactly, geometric effects can be inferred from the mechanics of pressure vessels. Compliance can be decreased by increasing hose thickness, reducing hose length, or reducing the internal hose diameter.

The simple calculations described above elucidate the geometric tradeoffs in the hydraulic transmission architecture. Because this application uses hydraulics differently from prior work, this model facilitates scaled designs for various applications and requirements. Transparency requires low friction, compliance, and inertia. From eqs. (14), (15) and (18), short and wide (large diameter) lines provide low friction and inertia. However, flexibility requires long and bendable (preferably small diameter) lines. Minimizing compliance requires using lines that are either materially rigid or thick-walled (and therefore unlikely to bend easily), or small in diameter and short. Design of line materials and geometry must include consideration of each of these requirements and the tradeoffs between them. Impedance can also be changed by altering the piston/cylinder geometry. Reducing the piston diameter can significantly reduce damping and inertia, as shown by Eqs. (14), (15) and (18), or permits smaller hose diameters for the same impedance properties, reducing compliance and improving flexibility. However, by Eq. (13) this increases the operating pressure, which has at least two negative consequences: greater part strength is required, and leakage is likely to increase, often requiring seals with greater friction. Thus changes in piston diameter can trade leakage and seal friction against reflected fluid friction and inertia.

Changes to system geometry improve certain aspects of performance at the expense of others. For any specific application the performance properties must be traded off against one another to find a suitable solution. Several rules of thumb should guide design:

1) To minimize reflected inertia, fluid friction, *and* compliance, the hydraulic line(s) should be made as large and radially rigid as possible.
2) Problem constraints should be used to determine how large, how heavy, and how rigid the line can be. These properties (related to flexibility) are traded against the endpoint impedance (transparency).
3) Decreasing the piston diameter decreases the reflected impedance but increases the operating pressure, and therefore the leakage rate and/or seal friction.

4.2 Proof of concept prototype and characterization

A prototype for the anti-gravity upper-limb application, shown in Fig. 8, was constructed to prove the concept of hybrid hydraulic actuation and to test the design model. A cogless tubular linear motor from Copley™, used previously as a version of the anti-gravity robot system, was selected as a source actuator for the system. A wound steel constant-force spring was used at each cylinder to apply the bias force. Springs are an advantageous means

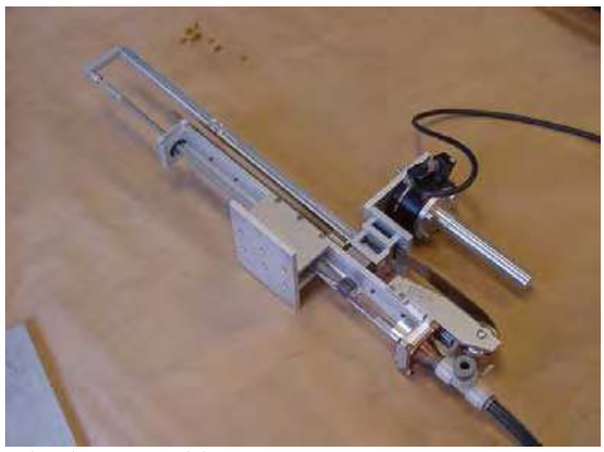

Fig. 10. Outer piston/cylinder assembly.

of applying a bias force because they contribute minimal inertia and friction. In choosing a working fluid for this application, fluid dynamics including the viscosity, density, and compressibility are especially important because they contribute to the endpoint impedance and haptic feel. Other factors (e.g. lubricity) that are important for other hydraulic applications are not important here because of the mechanical simplicity of the design. Water is cheap and available in abundance, and has minimal viscosity and compressibility with modest density. Water also poses minimal environmental threats (provided that it be separated from electrical and electronic equipment), and was therefore selected. The fittings that connect the flexible fluid line to solid structures are a critical component for design of a system with no small orifices. The analysis in 3.1 shows that losses from small orifices in servovalves lead to high endpoint impedance; the same can be said of orifices in a transmission line. Typical pipe and tube fittings generally obstruct the interior passages, greatly reducing diameter (and increasing damping) in a local area. In servo systems this effect is usually insignificant because the losses in the servovalve are so great as to dwarf fitting losses. For this application, however, an unobstructed fluid path is critical, and small orifices must be aggressively eliminated. Quick-release hose fittings that grip only the outside of the hose and leave the inside unobstructed were chosen for this prototype. To use such fittings, only hoses with relatively rigid walls are acceptable. A fuel hose meeting the SAE30R3 specification was selected. Perhaps the most challenging practical issue in hydraulic transmission design is the selection of moving seals with sufficiently low friction. In general, sliding seals require increased friction to reduce leakage. Because of the extreme low-friction needs of high-force haptic devices, static and Coulomb friction must especially be minimized. A wide array of seal types were considered, including elastomeric sliding seals, rolling diaphragm seals, bellows designs, and non-contacting seals. While rolling diaphragm seals show great promise, they generally provide a small ratio of travel to diameter. Non-contacting Airpot™ piston-cylinders were selected to minimize friction. This technology uses a precision ground sintered graphite piston that is diametrically matched to a high-precision glass tube to clearances that are generally between .0001" and .001". There is no physical seal, and the piston is designed to ride on a cushion of fluid between its outer edge and the cylinder's inner edge. This design minimizes friction but, because there is clearance between piston and cylinder, inevitably permits some leakage. Some amount of leakage of the working fluid across a low-friction seal is inescapable. When fluid leaks, the

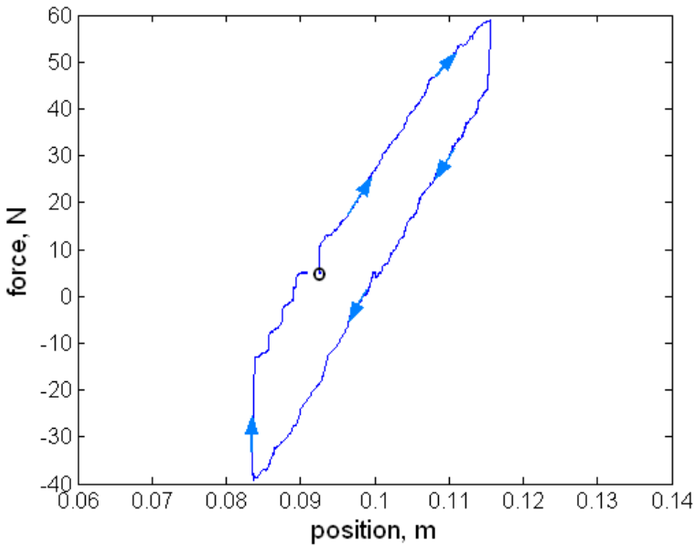

Fig. 11. Endpoint force versus position with virtual spring imposed, actuated by hand. The circle marks the start of the test and the arrows indicate the time course.

bias pressure prevents the replacement of the fluid with air. Instead the fluid volume is reduced. This is a positive feature of this bias pressure method; leakage produces a drift in endpoint position, but no significant change in dynamic transmission properties. To permit long-term operation, the leaked fluid must be replaced. For the prototype, a pump was used to replace leaked fluid. Because the pump is a high-impedance flow source, its supply rate is unaffected by changes in the transmission pressure, and it has a negligible impact on the system dynamics. Figure 10 shows the outer cylinder assembly.

Static and dynamic characterization tests were conducted to evaluate the prototype performance and validity of the design model. The force capacity, transmission stiffness, friction, inertia, weight and bandwidth were analyzed. The results are summarized and compared to the specification and the same quantities for a module based on the source actuator alone (Krebs et al., 2004) in Table 1.

	Specification	**Linear Motor**	**Passive Hydraulic Transmission**
Force capacity (N)	65	70	70
Endpoint weight (kg)	2	8.1	2.4
Core component weight (kg)	-	2.7	0.6
Endpoint inertia (kg)	2	2.7	4.5
Coulomb friction (N)	2	3.5	8
Stiffness (kN/m)	2	10	3.7

Table 1. Performance comparison of specifications, linear motor, and hydraulic transmission system for vertical therapy robot module. Improvement in weight is highlighted.

To determine the force capacity in tension and compression a high stiffness was commanded with the source actuator and a force was applied (and measured) at the

endpoint until saturation was reached. The transmission supported over 50 N in tension (exceeding the bias spring force) and almost 70 N in compression (meeting the saturation level of the source motor). The endpoint stiffness at DC is a series combination of the effective transmission stiffness and the source actuator stiffness. The source actuator controller was calibrated to achieve target endpoint stiffness using proportional motion feedback (simple impedance control). To determine the transmission stiffness, a virtual spring was imposed at the source actuator and the transmission endpoint force and position were measured as the endpoint was actuated slowly and steadily by hand. An example of the resulting data is shown in Fig. 11. The endpoint stiffness was determined from the slope of a linear fit to this data. The test was repeated at several different stiffnesses and the results were averaged, producing a measured transmission stiffness of 4020 N/m. When coupled to the source motor with maximum stiffness of 50,000 N/m, the resulting system can achieve stiffness up to 3700 N/m. This exceeds the specification by 85% and signals that radial hose flexibility does not prevent the creation of desired haptic sensations.

The endpoint friction profile was determined by measuring the force required to backdrive the system at constant speeds with a separate servo system. This test revealed approximately 8 N of Coulomb friction at the endpoint, in addition to viscous damping around 15 Ns/m. Coulomb friction appears as the separation between the upper and lower parts of the trace in Fig. 11. Approximately 3.5 N of Coulomb friction results from the source actuator, and the rest is mostly due to the bearings on the outer assembly. Significantly, a test on only the two pistons and the fluid, decoupled from mechanical bearings on each end, revealed less than 0.5 N friction from these critical parts. Viscous damping is approximately twice the estimate from the model. This results from viscous drag at the source motor as well as the fact that the transmission is not an ideal straight pipe, as modeled, and indicates a need for further model development to capture additional damping.

The model predicts over 2.5 kg of apparent fluid inertia, plus the inertia of the linear motor forcer and the moving hardware (handle, bearing carriage, sensors, etc.) in the endpoint package, totaling 4.9 kg. This significantly exceeds the 2 kg specification, because the design of this prototype erred on the side of making the hose extremely flexible yet radially stiff, and therefore very small. The most straightforward way to reduce inertia is by changing the hose geometry, as described in the previous section. A segmented line could help to balance hose flexibility and endpoint inertia. To measure the inertia, the source actuator was used to create a virtual spring. The transmission endpoint was displaced and released, creating an initial condition response. The transient of this response was fit with a second order initial condition response using the known endpoint stiffness. Inertia measured in several trials averaged to 4.5 kg. This is slightly less than the prediction because the inertia is actually partially distributed across a compliant part of the system (the transmission), while the model assumes a lumped mass with compliance originating only from the source actuator.

The weight of the endpoint package, including all parts of the assembly downstream of, but not including, the fluid line was 2.43 kg. Perhaps more importantly, the total weight of the (non-structural) components required to produce force (the cylinder, piston, piston rod assembly, fluid, and constant force spring assembly) was less than 630 g. By contrast, the weight of the linear motor magnet rod and forcer (for the same amount of travel) is over 2.7

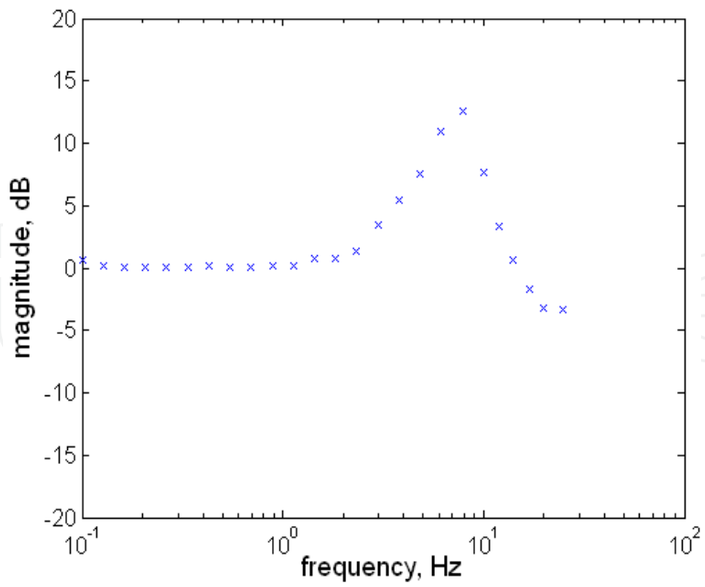

Fig. 12. Force magnitude output/input ratio versus frequency.

kg. The weight of the core technology to produce force, excluding bearings and structure, is reduced by approximately 77%—more than a factor of four. Additional weight reduction is achieved because the structure need not support such heavy core components.

Although not a direct performance requirement for this application, bandwidth was also measured by fixing the endpoint and commanding a sinusoidal force profile at various frequencies, with a magnitude of 12 N (approximately 20% of the peak force specification). A resulting plot of magnitude versus frequency is shown in Fig. 12. The system has a resonant peak around 8 Hz with a damping ratio between 0.1 and 0.2, and an open-loop bandwidth of approximately 20 Hz. The system geometry could easily be altered to increase viscous drag and reduce the resonant spike (e.g. by using more constrictive fittings) should this be desired. The bandwidth is more than adequate for human arm movement.

A critical assessment of the model's accuracy in predicting prototype impedance reveals moderate errors in the prediction of inertia, due to the assumption of lumped inertia in spite of the nonzero compliance, and somewhat larger errors in the prediction of damping, stemming primarily from the fact that damping is highly sensitive to tubing surface conditions, coiling, and interface losses. In general, over long stretches of tubing as implemented here, the primary goal is to keep friction below some level, rather than precisely achieve a specific value, so the simplified model suffices for this purpose. Prototype testing, along with the insights provided by the model, underscores the fact that seals are the core technology that determines performance. Smaller piston diameters can dramatically reduce apparent inertia and damping, but require higher pressures. At higher pressures, leakage increases unless seals are made tighter, which usually requires greater friction. It is clear from this work that improved seal technology that can better contain the fluid with minimal friction would substantially improve the capabilities of this technology.

4.3 Compliant Impedance Shaping

As discussed above, viscoelastic dynamics placed in series between a high-impedance actuator utilizing force feedback and the environment (termed series elasticity, mechanical

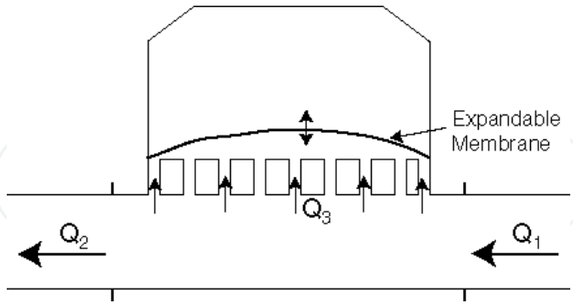

Fig. 13. Schematic of a cross-flow impedance shaper module.

filtering, or impedance shaping) can help to stabilize contact (Pratt & Williamson, 1995, Dohring & Newman, 2002). A passive hydraulic transmission can implement selected dynamic characteristics and is situated to place these dynamics in series, providing another potentially valuable aspect of this architecture. In the prototype described above, the source actuator friction and inertia contribute significantly to the endpoint impedance (half the friction and 1/3 the inertia), suggesting that it may be useful to use force feedback control around the actuator to reduce its apparent impedance, with series dynamics to improve coupled stability. An *impedance shaper* can be introduced to the transmission system to physically shape the dynamic characteristics of the actuator system as desired. A compliant impedance shaper (with compliance greater than that of the tubing alone) must introduce an alternative flow path so that the movement of each piston is not constrained absolutely by the movement of the other. A schematic depiction is shown in Fig. 13, where Q_1 and Q_2 represent the volumetric flow from each of the two pistons. Q_3 is the flow into or out of the impedance shaper. To make an impedance shaper with positive stiffness, there must be a means of expanding the volume in response to increases in fluid pressure (such as a flexible membrane). To endow the impedance shaper with dissipative behavior it suffices to regulate the geometry of the passages into and out of the stiffness chamber. In such simple and compact geometry, it is likely that damping can be more closely controlled and shaped than in the lengthy, flexible transmission line prototype. This architecture is dynamically analogous to a parallel spring and damper in series between the source actuator and the environment, as called for by Dohring and Newman (Dohring & Newman, 2002).

This simple impedance shaper can also introduce controlled inertia. The passageways can be designed to provide inertial forces that are proportional to the acceleration of the flow Q_3, the relative flow between Q_1 and Q_2, rather than the acceleration of either piston. The damping and inertia can be regulated independently either by varying both the diameter and length of the passageways, or by introducing obstructions of negligible length (e.g. small holes) that increase damping but not inertia. More complex dynamics can be designed using simple fluid circuits if advantageous. The passive hydraulic transmission provides a platform where desired dynamics can be implemented and adjusted with simple, lightweight physical structures. Aside from moving seals, hydraulic system dynamics are generally devoid of backlash, discontinuous nonlinear friction, and other "hard"

nonlinearities, and physical laws that govern behavior are well understood. The benefits of impedance shaping can be added to remote power transmission and intrinsic gearing in an integrated package to improve high-force, low-impedance robot actuation capabilities.

5. Conclusions

This chapter presented and defined high force haptic systems, and articulated the specific constraints that make the selection of actuators for this application difficult. To provide context, the pioneering high force haptics application of therapeutic robotics, and the obstacles to continued advancement of the field, were discussed. We continue to develop therapeutic robots for human movement from lower body (including partial weight support) to fine finger motions, and the actuation problem is the core engineering challenge for almost all of the designs. Major actuation and control technologies suitable for human-scale interaction were explored and evaluated for their fitness for high force haptics. As existing technology does not meet all of the needs of this field, we described our development and proof-of-concept of a hybrid hydraulic actuation scheme. This approach exploits the high force density of hydraulic systems without producing inevitably high endpoint impedance. Though analogous to mechanical transmissions, the hydraulic approach enables a dramatically more flexible coupling between source actuators and interaction ports. The simplicity of this design architecture, and the relatively straightforward and validated impact of geometric design parameters, makes it amenable to scaling for use as modular actuators in robots of all shapes and sizes. With this architecture, a single integrated physical system, the passive hydraulic transmission, can provide remote power transmission (directly reducing endpoint actuator weight), intrinsic gear reduction (permitting variation in actuator sizing) and impedance shaping (stabilizing contact while more aggressive force feedback is used). The structure of hybrid hydraulic actuators may also permit operation in environments that are hostile to other actuator types, including near or inside medical neuroimaging equipment for use in concert with, for instance, functional magnetic resonance imaging (fMRI). Together with existing actuator and interaction control technology, as well as developing new capabilities for advanced interactive actuators, the hybrid hydraulic actuation approach contributes to a diverse and expanding suite of tools for addressing the high force haptics challenge. As a one-size-fits-all solution to this formidable challenge seems unlikely to emerge, the growing community of high force haptics researchers should consider each of these possible solutions for their applications and select those best suited to their needs.

Acknowledgements

Support: NDSEG Fellowship, NIH HD37397, Burke Medical Research Institute, New York State C019772.

6. References

Bar-Cohen, Y. (Ed.) (2004). *Electroactive Polymer (EAP) Actuators as Artificial Muscles: Reality, Potential, and Challenges.* SPIE Press, Bellingham, WA.

Berkelman, P., Butler, Z. & Hollis, R. (1996). Design of a Hemispherical Magnetic Levitation Haptic Interface Device. *Proc. ASME Int Mech Eng Cong Expo,* Vol. 58, pp. 483-488.

Biggs, S. & Srinivasan, M. (2002). Haptic Interfaces, In: *Handbood of Virtual Environments*, Stanney, K. (Ed.), pp. 93-115, Lawrence Erlbaum Associates, Inc., New Jersey.

Buerger, S. & Hogan, N. (2007). Complementary Stability and Loop-Shaping for Improved Human-Robot Interaction. *IEEE Trans Rob Autom,* Vol. 23, pp. 232-244.

Buerger, S., Krebs, H. & Hogan, N. (2001). Characterization and Control of a Screw-Driven Robot for Neurorehabilitation. *Proc. IEEE CCA / ISIC.*

Carignan, C. & Cleary, K. (2000). Closed-Loop Force Control for Haptic Simulation of Virtual Environments. *Haptics-e,* Vol. 1, No. 2, pp. 1-14.

Colgate, J. & Hogan, N. (1988). Robust Control of Dynamically Interacting Systems. *Int J Contr,* Vol. 48, pp. 65-88.

Dohring, M. & Newman, W. (2002). Admittance Enhancement in Force Feedback of Dynamic Systems, *Proc. IEEE ICRA,* pp.638-643.

Goldfarb, M., Barth, E., Gogola, M. & Wehrmeyer, J. (2003). Design and Energetic Characterization of a Liquid-Propellant-Powered Actuator for Self-Powered Robots. *IEEE / ASME Trans Mechatronics,* Vol. 8, pp. 254-262.

Guizzo, E. & Goldstein, H. (2005). The Rise of the Body Bots. *IEEE Spectrum*, Vol. 42, pp. 50-56.

Hidler, J., Nichols, D., Pelliccio, M., Brady, K., Campbell, D. D., Kahn, J. H., and Hornby, T. G. (2009). Multicenter Randomized Clinical Trial Evaluating the Effectiveness of the Lokomat in Subacute Stroke. *Neurorehabilitation and Neural Repair* Vol. 23**,** pp. 5-13.

Hogan, N. & Buerger, S. (2005). Impedance and Interaction Control, In: *Robotics and Automation Handbook*, Kurfess, T. (Ed.), ch. 19, CRC Press, New York.

Hogan, N. (1985). Impedance Control: An Approach to Manipulation. *ASME J Dyn Sys Meas Contr,* Vol. 107, pp. 1-24.

Hogan, N. (1989). Controlling Impedance at the Man/Machine Interface, *Proc. IEEE ICRA,* pp. 1626-1631.

Hogan, N., Krebs, H. I., Rohrer, B., Palazzolo, J. J., Dipietro, L., Fasoli, S. E., Stein, J., Hughes, R., Frontera, W. R., Lynch, D., and Volpe, B. T. (2006). Motions or muscles? Some behavioral factors underlying robotic assistance of motor recovery *Journal Of Rehabilitation Research And Development* Vol. 43**,** pp. 605-618.

Hollerbach, J., Hunter, I. & Ballantyne, J. (1992). A Comparative Analysis of Actuator Technologies for Robotics, In: *The Robotics Review 2,* Khatib., O. (Ed.), pp. 299-342, MIT Press, Cambridge, MA.

Hornby, T. G., Campbell, D. D., Kahn, J. H., Demott, T., Moore, J. L., and Roth, H. R. (2008). Enhanced Gait-Related Improvements After Therapist- Versus Robotic-Assisted Locomotor Training in Subjects With Chronic Stroke: A Randomized Controlled Study. *Stroke* Vol. 39**,** pp. 1786-1792.

Israel, J. F., Campbell, D. D., Kahn, J. H., and Hornby, T. G. (2006). Metabolic Costs and Muscle Activity Patterns During Robotic- and Therapist-Assisted Treadmill Walking in Individuals with Incomplete Spinal Cord Injury. *Physical Therapy* Vol 86**,** pp. 1466.

Kazerooni, H. & Guo, J. (1993). Human Extenders. *ASME J Dyn Sys Meas Contr,* Vol. 115, pp. 281-290.

Krebs, H. I., Ladenheim, B., Hippolyte, C., Monterroso, L., and Mast, J. (2009). Robot-assisted task-specific training in cerebral palsy. *Developmental Medicine and Child Neurology* Vol. 51**,** pp. 140-145.

Krebs, H. I., Palazzolo, J. J., Dipietro, L., Volpe, B. T., and Hogan, N. (2003). Rehabilitation robotics: Performance-based progressive robot-assisted therapy. *Autonomous Robots* Vol. 15**,** pp. 7-20.

Krebs, H., Ferraro, M., Buerger, S., Newbery, M., Makiyama, A., Sandmann, M., Lynch, D., Volpe, B. & Hogan, N. (2004). Rehabilitation Robotics: Pilot Trial of a Spatial Extension for MIT-MANUS. *J NeuroEng Rehab.* Vol 1, p. 5.

Kwakkel, G., Kollen, B. J., and Krebs, H. I. (2007). Effects of Robot-assisted therapy on upper limb recovery after stroke: A Systematic Review. *Neurorehabilitation and Neural Repair*.

Lawrence, D. (1993). Stability and Transparency in Bilateral Teleoperation. *IEEE Trans Rob Autom,* Vol. 9, pp. 624-637.

Lee, Y. & Ryu, D. (2008). Wearable Haptic Glove Using Micro Hydraulic System for Control of Construction Robot System with VR Environment. *Proc. IEEE Int Conf on Multisensor Fusion and Integration for Intelligent Systems,* pp. 638-643.

Massie, T. & Salisbury, K. (1994). The PHANTOM Haptic Interface: A Device for Probing Virtual Objects. *Proc. ASME Winter Annual Meeting, Symposium on Haptic Interfaces for Virtual Environment and Teleoperator Systems.*

McBean, J. & Breazeal, C. (2004). Voice Coil Actuators for Human_Robot Interaction. *Proc. IEEE/RSJ Int Conf on Intel Rob Sys,* pp. 852-858.

Neckel, N. D., Blonien, N., Nichols, D., and Hidler, J. (2008). Abnormal joint torque patterns exhibited by chronic stroke subjects while walking with a prescribed physiological gait pattern. *Journal of NeuroEngineering and Rehabilitation* Vol. 5**,** pp. 1-13.

Newman, W.S. (1992). Stability and Performance Limits of Interaction Controllers. *ASME J Dyn Sys Meas Contr,* Vol. 114, pp. 563-570.

Nudo, R. J. (2007). Postinfarct Cortical Plasticity and Behavioral Recovery. *Stroke* Vol. 38**,** pp. 840-845.

Peshkin, M., Colgate, J., Wannasuphoprasit, W., Moore, C., Gillespie, R. & Akella, P. (2001). Cobot Architecture. *IEEE Trans Rob Autom,* Vol. 17, pp. 377-390.

Prange, G. B., Jannink, M. J. A., Groothuis-Oudshoorn, C. G. M., Hermens, H. J., and Ijzerman, M. J. (2006). Systematic review of the effect of robot-aided therapy on recovery of the hemiparetic arm after stroke. *Journal of Rehabilitation Research and Development* Vol. 43**,** pp. 171-184.

Pratt, G. & Williamson, M. (1995). Series Elastic Actuators. *Proc. IEEE/RSJ Int Conf on Human Robot Interaction and Cooperative Robots,* pp. 399-406.

Roberts, M. H. (2004). "A Robot for Gait Rehabilitation." Massachusetts Institute of Technology.

Roy, A., Krebs, H. I., Williams, D. J., Bever, C. T., Forrester, L. W., Macko, R. M., and Hogan, N. (2009). Robot-Aided Neurorehabilitation: A Novel Robot for Ankle Rehabilitation. *IEEE Transactions on Robotics* Vol. 25, pp. 569-582.

Taub, E., and Uswatte, G. (2006). Constraint-Induced Movement therapy: Answers and questions after two decades of research. *NeuroRehabilitation* Vol. 21**,** pp. 93-95.

Tondu, B. & Lopez, P. (2000). Modeling and Control of McKibben Artificial Muscle Robot Actuators. *IEEE Contr Sys Magazine,* Vol. 20, Issue 2, pp. 15-38.

Townsend, W. & Guertin, J. (1999). Teleoperator Slave – WAM Design Methodology. *Ind Robot,* Vol. 26, p. 167.

Tressler, J., Clement, T., Kazerooni, H. & Lim, A. (2002). Dynamic Behavior of Pneumatic Systems for Lower Extremity Extenders. *Proc IEEE ICRA,* pp. 3248-3253.

Veneman, J. F., Kruidhof, R., Hekman, E. E. G., Ekkelenkamp, R., Asseldonk, E. H. F. V., and Kooij, H. v. d. (2007). Design and Evaluation of the LOPES Exoskeleton Robot for Interactive Gait Rehabilitation. *IEEE Transactions on Neural Systems and Rehabilitation Engineering* Vol. 15, pp. 379-386.

Volpe, B. T., Ferraro, M., Lynch, D., Christos, P., Krol, J., Trudell, C., Krebs, H. I., and Hogan, N. (2004). Robotics and Other Devices in the Treatment of Patients Recovering Stroke. *Current Atherosclerosis Reports* Vol. 6, pp. 314-319.

Volpe, B. T., Huerta, P. T., Zipse, J. L., Rykman, A., Edwards, D., Dipietro, L., Hogan, N., and Krebs, H. I. (2009). Robotic Devices as Therapeutic and Diagnostic Tools for Stroke Recovery. *Archives Of Neurology* Vol. 66, pp. 1086-1090.

Wolf, S. L., Winstein, C. J., Miller, J. P., Taub, E., Uswatte, G., Morris, D., Giuliani, C., Light, K. E., and Nichols-Larsen, D. (2006). Effect of Constraint-Induced Movement Therapy on Upper Extremity Function 3 to 9 Months After Stroke: The EXCITE Randomized Clinical Trial. *Journal of the American Medical Association* Vol. 296, pp. 2095-2104.

Wyatt, J., Chua, L., Gannett, J., Goknar, I. & Green, D. (1981). Energy Concepts in the State-Space Theory of Nonlinear n-ports: Part I – Passivity. *IEEE Trans Circ Sys*, Vol. 23, pp. 48-61.

IntechOpen

Advances in Haptics

Edited by Mehrdad Hosseini Zadeh

ISBN 978-953-307-093-3
Hard cover, 722 pages
Publisher InTech
Published online 01, April, 2010
Published in print edition April, 2010

Haptic interfaces are divided into two main categories: force feedback and tactile. Force feedback interfaces are used to explore and modify remote/virtual objects in three physical dimensions in applications including computer-aided design, computer-assisted surgery, and computer-aided assembly. Tactile interfaces deal with surface properties such as roughness, smoothness, and temperature. Haptic research is intrinsically multi-disciplinary, incorporating computer science/engineering, control, robotics, psychophysics, and human motor control. By extending the scope of research in haptics, advances can be achieved in existing applications such as computer-aided design (CAD), tele-surgery, rehabilitation, scientific visualization, robot-assisted surgery, authentication, and graphical user interfaces (GUI), to name a few. Advances in Haptics presents a number of recent contributions to the field of haptics. Authors from around the world present the results of their research on various issues in the field of haptics.

InTech Europe
University Campus STeP Ri
Slavka Krautzeka 83/A
51000 Rijeka, Croatia
Phone: +385 (51) 770 447
Fax: +385 (51) 686 166
www.intechopen.com

InTech China
Unit 405, Office Block, Hotel Equatorial Shanghai
No.65, Yan An Road (West), Shanghai, 200040, China
中国上海市延安西路65号上海国际贵都大饭店办公楼405单元
Phone: +86-21-62489820
Fax: +86-21-62489821

IntechOpen